YURIY NATANZON*, ZBIGNIEW ŁODZIANA*

QUANTUM MECHANICAL CALCULATIONS OF ELASTIC PROPERTIES OF DOPED TETRAGONAL YTTRIA-STABILIZED ZIRCONIUM DIOXIDE

We report first principles calculations of the electronic and elastic properties of yttria-stabilized tetragonal zirconium dioxide doped with metal oxides like: GeO_2, TiO_2, SiO_2, MgO and Al_2O_3. It is shown that addition of such dopants affects selected elastic properties of ZrO_2, which is driven by the attraction of electron density by dopant atom and creation of stronger dopant–oxygen bonds. This effect contributes to the increase of superplasticity of doped material.

Keywords: *Y-stabilized zirconia, superplasticity, net charge,* ab initio *calculations*

KWANTOWO-MECHANICZNE OBLICZENIA WŁASNOŚCI ELASTYCZNYCH FAZY TETRAGONALNEJ DWUTLENKU CYRKONU STABILIZOWANEGO TLENKIEM ITRU

W pracy przedstawione są wyniki kwantowo-mechanicznych obliczeń własności elektronowych i elastycznych fazy tetragonalnej dwutlenku cyrkonu stabilizowanego tlenkiem itru z domieszkami tlenków metali, takich jak GeO_2, TiO_2, SiO_2, MgO oraz Al_2O_3. Pokazano, że domieszkowanie wpływa na wybrane stałe elastyczne ZrO_2, co jest spowodowane zmianami rozkładu gęstości elektronowej w pobliżu atomu domieszki oraz kreacją silniejszego wiązania domieszka–tlen. Ten efekt wnosi wkład do zwiększenia nadplastyczności domieszkowanego materiału.

Słowa kluczowe: *dwutlenek cyrkonu, nadplastyczność, ładunek atomowy, obliczenia ab initio*

1. Introduction

Zirconium oxide (ZrO_2) is a solid ceramic material which is used as an ionic conductor in solid oxide fuel cells [1], as a refractory material [2], or as a substitution for diamond [3]. Fine grained zirconium oxide ceramics are known for its extreme superplastic properties – doped zirconia may undergo deformation above 200% of its initial length. These properties were an active field of research during the last decade (see e.g. review [4]). Many experiments show that the doping of Y-stabilized ZrO_2

---

*Henryk Niewodniczański Institute of Nuclear Physics Polish Academy of Sciences, Krakow, Poland, Yuriy.Natanzon@ifj.edu.pl, Zbigniew.Lodziana@ifj.edu.pl

with different metal oxides such as GeO_2, TiO_2, SiO_2, MgO and Al_2O_3 and others strongly increase the superplasticity of the material [4, 5, 6, 7, 8].

Existing (and most widely accepted) explanation include the sliding of grains at the boundary driven by dopant cation segregation on the boundary as originally proposed by Berbon and Langon [9]. Another theoretical explanation has been proposed recently by A. Kuwabara *et al.* [5] using GeO_2 and TiO_2 dopants. They related changes in theoretically computed changes in net ionic charges of cations and anions with experimentally measured reduction of superplastic stress flow. This phenomenon is not yet completely understood at atomic level.

ZrO_2 is an insulator with a band gap of $4.2\,eV$ [10, 11]. Main structural polymorphs of ZrO_2 include the high temperature cubic (2650–2990 K) and tetragonal (1400–2650 K) phases. The monoclinic phase exists at the temperatures below 1400 K. The high temperature phases can be stabilized with a small amount of yttria (Y_2O_3). As seen from the phase diagram of Y-stabilized zirconia (YZP) in Ref.[12], the tetragonal phase of zirconia exists at yttria concentrations below $6\,mol\%$ and temperature range of about 600–2000 K. In this paper we consider tetragonal zirconia with the concentration of yttria of 0–$4.3\,mol\%$.

Our intention in this study is to gain more detailed microscopic insight into the superplasticity of Y-stabilized tetragonal phase of ZrO_2 doped with different metal oxides. To achieve this we have carried out series of quantum mechanical calculations of elastic and electronic properties of zirconia with various dopants.

2. Model and method of calculation

Simultaneous atomistic calculations of elastic and fine electronic properties require advanced quantum methods to describe efficiently systems consisting of hundred or more atoms. The present calculations were performed within density-functional theory (DFT) [13] with generalized-gradient approximation (GGA) [14] for exchange-correlation functional. The linear combination of atomic orbitals (LCAO) basis set was used, as implemented in the SIESTA program [15].

In the present studies the supercell technique was used to mimic various concentration of yttrium and other dopants. At the first step, experimental unit cell parameters of ZrO_2 were optimized. The calculated lattice constants are $a = b = 3.61\,Å$, $c = 5.20\,Å$ that compare well with experimental data $a = b = 3.60\,Å$, $c = 5.18\,Å$ [19]. The tetragonal phase of ZrO_2 has the space group symmetry $P4_2/nmc$ [20], with the atomic positions (0.0, 0.0, 0.0) for Zr and $(0, \frac{1}{2}, 0.2)$ for O. The optimized unit cell was multiplied in selected directions to obtain a desired size of the supercell. In each supercell we replaced two Zr atoms in (a, b) plane with Y and one oxygen atom was removed to provide a correct stoichiometry. Dopant metal oxides were introduced in the same way, so each supercell contains one molecular unit of Y_2O_3 and one molecular unit of dopant oxide. The concentrations of Y and dopant oxides were the same depending on the size of the supercell (the smaller the cell the larger the concentration and vise versa). Such an approach has limitations on the possible

dopant concentrations as we can only change it in a defined finite steps. The selected Y/dopant concentration that were considered are shown in Table 1.

Because of the difficulty of introducing aliovalent dopant metal oxides (Al_2O_3 and MgO) into ZrO_2 only the electronic properties were calculated for these dopants and only for the concentration of 2.8 mol%.

Table 1

Model supercells used in calculations and the corresponding Y/dopant concentrations. The supercell size is shown in terms of the unit cell

Supercell size	Number of atoms	Number of valence electrons	Y/dopant concentration, mol%
3×2×2	71	568	4.3
3×3×2	107	856	2.8
3×3×3	161	1288	1.9

Several mutual locations of host ZrO_2 atoms and dopant atoms were tested and the energetically most stable configuration is for Y atoms located in the (a, b) plane with the oxygen vacancy located as the first neighbor of dopants. Such configuration is in agreement with previous calculations by Bogicevic *et al.* [12] and Eichler [10]. The distance between Y atoms is 3.5 Å and the distance between Y atom and the position of the oxygen vacancy is 2.13 Å. However, after oxygen removal the actual vacancy position was changed but it is not difficult to determine it explicitly.

For each dopant concentration and for each supercell size we have performed the full structural relaxation (the supercell size and atomic positions within the supercell) to obtain the ground state configuration of the system. The conjugate-gradients method was used for such an optimization [22].

3. Numerical techniques and performance optimization of SIESTA

The SIESTA program is one of the fastest among DFT codes and that's why it has been chosen for our calculations. The numerical techniques implementation of DFT used there makes use of specific methods to speed up the calculations and balance between the desired accuracy and calculation time. First, only the valence electrons which take part in bond formation are considered. The other electrons (also called "core electrons") are replaced by effective norm-conserving potentials with Troullier and Martins parametrization [23]. In this calculation we have used GGA pseudopotentials in Perdew-Burke-Ernzerhof parametrization [24]. In order to achieve a better accuracy we have also treated some core electrons as valence. Thus the valence electron configuration was $4s^24p^65s^24d^2$ for Zr, $4s^24p^65s^24d^1$ for Y, $3s^23p^64s^23d^2$ for Ti, $3s^23p^2$ for Si, $4s^24p^2$ for Ge, $3s^23p^1$ for Al and $3s^2$ for Mg.

Second, all integrals are calculated on the finite real space grid. The continuous electron density within a periodic supercell is represented on the finite grid with the grid density determined by the plane wave cutoff. A plane-wave cutoff of 476 eV (350 Ry) was used in this calculation and a k point grid with a step of 0.03 Å. The second grid over k-points is required to sample the electronic density in the Brillouin zone of reciprocal space. The smoothness of the the density determines the density of the grid required for a given accuracy. The use of pseudopotential significantly reduces memory requirements, as the rapidly varying quantities near the ionic cores are replaced by smooth functions [15]. The wave functions in SIESTA are expanded into a linear combination of atomic orbitals (LCAO) that consists of the localized radial part and spherical functions. Such orbitals go to zero beyond a defined cutoff radius. This provides an additional speed advantage over other DFT (plane wave) codes. The important approach used in SIESTA is calculations of the matrix elements of the Kohn-Sham Hamiltonian. They are calculated in such a way that the terms involving integrals over two atoms are calculated a priori and stored as the tables to be interpolated whenever the spacing between atoms varies. All other terms are calculated on the grid, as described above [15, 16]. Such a representation provides the electron density in the form of 3-dimensional matrices that allow implementation of various optimized linear algebra numerical procedures [15]. The sparse matrix multiplication techniques and fast Fourier transform for calculating the necessary integrals were used [15].

All the parts of the SIESTA code are written using the strategy of distributing data over the nodes, thus it can be used for parallel calculation. In our work we have used the k-point parallelization which is recommended for the systems with a large number of k points and relatively small overlap matrices. In this process the integrals on different k points are calculated on different nodes. It is effective when the number of k points is proportional to the number of available nodes. As we have used 2 and 4 processor nodes mainly, we have used from 8 to 24 k points depending on the size of the supercell. SIESTA uses MPI interface for parallelization. The communication between the nodes is done using the BLACS library which is built on top of MPI [17]. For parallel calculation of matrix elements, SCALAPACK library functions are used.

The effective numerical algorithms implemented in SIESTA allow a linear scaling of the calculation time with the increase in the system size. This allowed us to use different supercells containing from 71 to 161 atoms without a significant increase on the computation time and demand for computer resources.

The calculations were performed at ACK CYFRONET AGH using SGI Altix 3700 computer. As SIESTA is written mainly in Fortran90, it was possible to increase the performance by using Intel Fortran compiler which produces a code optimized for Intel processors. O2 optimization flag was used for compilation. As most mathematical operations were implemented through the standard functions in the BLAS and LAPACK mathematical libraries, it was possible to use Intel Math Kernel Libraries pack instead. According to the results of several performance tests, the calculations using 4 processors run approximately twice faster than a serial computation on Intel

Core 2 Duo workstation (for the system of 40-160 atoms.) The same performance is achieved by other researchers using SIESTA reported in private communications and on SIESTA mail list.

4. Results and discussion

The phenomenon of superplasticity is related to changes of the macroscopic elastic properties of the ZrO_2. Since it is attributed to the grain boundary sliding elastic properties of the single crystal grains are usually not considered as an important factor that affects the plastic properties of YZP. However, it is well known that dopant concentration increases at the grain boundary, thus concentration dependent elastic properties might be related directly to superplasticity. The basic elastic properties include volume compressibility (bulk modulus) and tensor of the elastic constants. Below we present how these properties change with changing concentration of dopants.

4.1. Bulk modulus

Bulk modulus is a measure of material's response to the uniform volume deformation. Bulk modulus was calculated by series of the supercell deformations in the range of -3% to 3% of its initial volume with the step of 0.5%. For each deformation the atomic positions within the supercell were relaxed and the total energy of the system was calculated. To obtain the value of bulk modulus the dependence of the total energy E of the system on the supercell volume V was fitted by Murnaghan equation of state [18]:

$$E = E_0 + \frac{B_0}{B_0'} V \left(\frac{(V_0/V)^{B_0'}}{B_0' - 1} + 1 \right) - \frac{B_0 V_0}{B_0' - 1},$$

where E_0 is the total energy of the ground state configuration of the cell of volume V_0, B_0 is the equilibrium bulk modulus (at external pressure $P = 0$), and $B_0' = \left(\frac{\partial B}{\partial P} \right)_T = const$ is the derivative of bulk modulus.

The bulk modulus was calculated for Ge, Ti and Si dopants and for each of dopant concentration. The dependence of bulk modulus on Y/dopant concentration is presented in Figure 1. One can see, that there is no systematic change of B_0 with Y/dopant addition. The fluctuations are related to the accuracy of calculations.
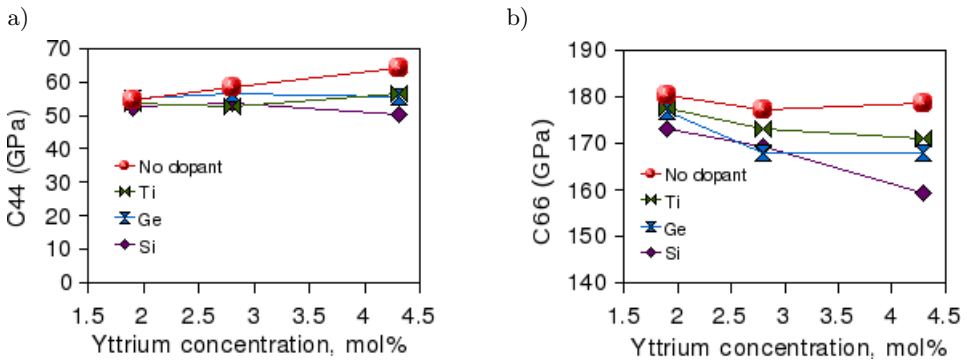
4.2. Shear elastic constants

Various models of the superplastic behavior of doped ZrO_2 indicate that the macroscopic grain deformation is not related to the increase of supeplasticity [4]. This is in good agreement with weak concentration dependence of the bulk modulus as shown in the previous section. However, analysis of the components of the elastic constants can reveal more detailed information about system response to nonuniform strains that arise during grain sliding.
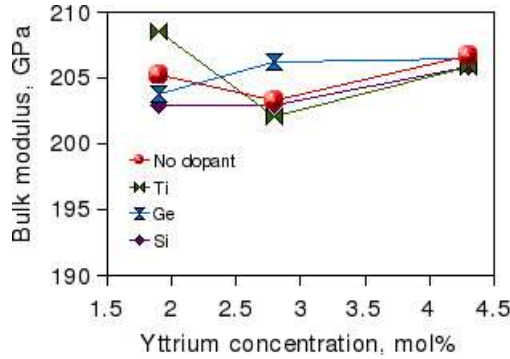
Fig. 1. Dependence of bulk modulus of ZrO_2 on Y/dopant concentration. Lines are shown as a guide for the eyes

Shear elastic constants C_{44} and C_{66} of doped ZrO_2 were calculated by series of finite deformations of the supercell. For each constant and each dopant concentration the appropriate shear deformation of 1% was applied and the components of the stress tensor were calculated. For each deformation a full relaxation of the atomic positions in the supercell was performed. The C_{44} and C_{66} elastic constants are presented in Figure 2.

a)

b)

Fig. 2. C_{44} elastic constant (a) and C_{66} elastic constant of ZrO_2 (b) as functions of Y/dopant concentration. Red line with right-oriented triangles correspond to undoped Y-stabilized ZrO_2, other symbols correspond to the system with dopant metal oxides. Lines are shown as a guide for the eyes

As can be seen in the Figure 2(b) a reduction of the C_{66} elastic constant is observed and correlated with dopant concentration. Such a dependence is well correlated with the decrease of superplastic flow stress observed experimentally.

Rapid decrease of C_{66} elastic constant with increasing dopant concentration indicates that at the grain boundary a pronounced shear deformation can be observed.

Thus if one considers grains of polycrystalline ZrO_2 sliding in this direction, one can see that boundary sliding can be affected by crystalline deformation. The concentration of dopants is larger at the boundary than in the bulk. This phenomena would contribute to the overall superplasticity of ZrO_2.

4.3. Net ionic charges

Net ionic charge describe the real charge of the atom in a molecule or crystal. The formal oxidation state of Zr in zirconia is $+4e$ and for O it is $-2e$. The net charge describes charge transfer between Zr and O in Zr–O bond. The net charge in this study was calculated by explicit integration of the electron density around each atom over a sphere of radius $1.2\,\text{Å}$ for Zr and O, $1.16\,\text{Å}$ for Y, $1\,\text{Å}$ for Ti, Ge, Si, Al and Mg. The calculated net ionic charges are presented in Figure 3.
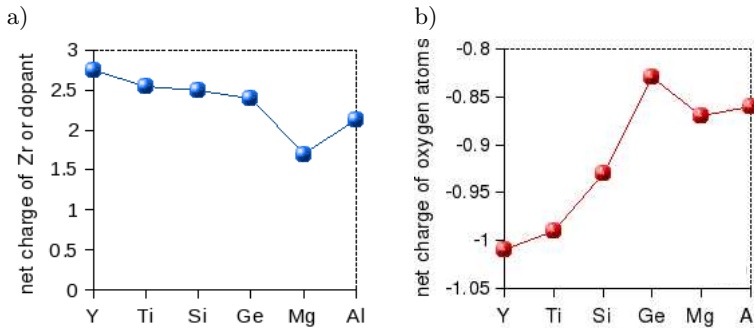
Fig. 3. Net ionic charges of Zr and dopant cations (a) and oxygen atoms of minimum ionicity (b) for $2.8\,\text{mol}\%$ doped Y-stabilized ZrO_2. Lines are shown as a guide for the eyes

One can see that net charges of zirconium and dopants are in agreement with their Pauling electronegativities, thus dopant atoms have lower ionicity than Zr and Y. Both the lowest and the highest oxygen ionicity in a unit cell decrease (their absolute values). This indicates that a dopant atom attracts adjacent oxygen to create stronger dopant–oxygen bonds than in pure zirconia. This also influences nearby Zr atoms and Zr–O bonds weaken.

The observed changes of the ionicity have only local character and do not depend on the dopant concentration below $5\,\text{mol}\%$.

5. Conclusion

The SIESTA is a fast and efficient DFT code for calculation of electronic and elastic properties of materials which was written for parallel calculations and thus can make use of modern supercomputers like those at ACK CYFRONET AGH. It uses numerical techniques which allows linear scaling of the computation time with the increase of the system size. Our performance tests have shown that the calculations

with 4 processors run approximately twice faster than a serial computation on Intel Core 2 Duo workstation (for the system of 40- -160 atoms.). Such performance is comparable to the one achieved by other researchers using SIESTA and reported in private communications and on SIESTA mail list.

The results of calculations performed reveal a new mechanism which besides the other effects (e.g. temperature, cation diffusion, grain boundary sliding etc) contributes to the superplasticity increase in ZrO_2, i.e. the decrease of shear elastic constants after dopant addition. Shear elastic constants decrease with the increase of dopant concentration (until the phase transition to the cubic phase takes place) so to obtain the maximum ductility, the most possible Y/dopant concentration for this phase (which is approximately 6 mol% for tetragonal zirconia) should be used. On the other hand, it was shown that as bulk modulus does not significantly change after dopant addition, uniform volume deformation doesn't contribute to the increase of superplasticity.

Our calculations are in agreement with the results of Kuwabara *et al.* [5] which relate changes in net ionic charges with the increase of tensile ductility of the material. As dopant atom has lower ionicity than Zr and Y, stronger dopant–oxygen bonds are created. This attracts oxygens and causes the creation of weaker Zr–O bonds near the dopant than those in an undoped system. This results in the overall increase in elasticity and superplasticity.

Acknowledgments

References

[1] Singhal S. C.: *Advances in solid oxide fuel cell technology.* Solid State Ionics **135**, 305 (2000)

[2] Zhou N., Liu J., Lin B.: *Refractory raw materials in China.* American Ceramic Society Bulletin **84**, 20 (2005)

[3] Schwartz M. M.: *Encyclopedia of Materials, Parts, and Finishes.* CRC Press (2002), p. 888

[4] Jimenez-Melendo M., Dominiguez-Rodriguez A., Bravo-Leĺn A.: *Superplastic Flow of Fine-Grained Yttria-Stabilized Zirconia Polycrystals: Constitutive Equation and Defromation Mechanisms.* J. Am. Cem. Soc. **81**, 2761 (1998)

[5] Kuwabara A., Nakano M., Yoshida H., Ikuhara Yu., Sakuma T.: *Superplastic flow stress and electronic structure in yttria-stabilized tetragonal zirconia polycrystals doped with GeO_2 and TiO_2.* Acta Materialia **52**, 5563 (2004)

[6] Hiraga K.: *Development of High-Strain-Rate superplastic Oxide Ceramics.* Journal of the Ceramic Society of Japan **115**, 395 (2007)

[7] Yoshida H.: *Doping dependence of High Temperature Plastic Flow Behaviour in TiO_2 and GeO_2-doped Tetragonal ZrO_2 Polycrystals.* Journal of the Ceramic Society of Japan **114**, 155 (2006)

[8] Sakka Y., Suzuki T. S., Matsumoto T., Morita K., Hiraga K., Moriyoshi Y.: *Effect of titania and magnesia addition to 3 mol% yttria doped tetragonal zirconia on some diffusion related phenomena.* Solid State Ionics **172**, 499 (2004)

[9] Berbon M. Z., Langdon T. G.: *An examination of the flow process in superplastic yttria-stabilized tetragonal zirconia.* Acta Materialia **47**, 2485 (1999)

[10] Eichler A.: *Tetragonal Y-doped zirconia: Structure and ion conductivity.* Phys. Rev. B **64**, 174103 (2001)

[11] McComb D. W.: *Bonding and electronic structure in zirconia pseudopolymorphs investigated by electron energy-loss spectroscopy.* Phys. Rev. B **54**, 7094 (1996)

[12] Bogicevic A., Wolverton C., Crosbie G. M., Stechel E. B.: *Defect ordering in aviovalently doped cubic zirconia from first principles.* Phys. Rev. B **64**, 014106 (2001)

[13] Kohn W., Sham L. J.: *Self-consistent Equations Including Exchange and Correlation Effects.* Phys. Rev. **140**, 1133 (1965)

[14] Perdew J. P., Chevary J. A., Vosko S. H., Jackson K. A., Pederson M. R., Singh D. J., Fiolhais C.: *Atoms, molecules, solids, and surfaces: Applications of the generalized gradient approximation for exchange and correlation.* Phys. Rev. B. **46**, 6671 (1992).

[15] Soler J., Artacho E., Gale J. D., García A., Junquera J., Ordejón P., Sánchez-Portal D.: *The SIESTA method for ab initio order-N materials simulation.* J. Phys.: Condens. Matter **14**, 2745 (2002)

[16] Ordejón P., Sánchez-Portal D., García A., Artacho E., Junquera J., Soler J.: *Large scale DFT calculations with SIESTA.* RIKEN Review **29**, 42 (2000)

[17] Artacho E., Gale J. D., García A., Junquera J., Martin R. M., Ordejón P., Sánchez-Portal D., Soler J.: *SIESTA 2.0. User's Guide.* Available from `http://www.uam.es/siesta`

[18] Murnaghan F. D.: *The Compressibility of Media under Extreme Pressures.* Proceedings of National Academy of Sciences **30**, 244 (1944)

[19] Howard C. J., Hill R. J., Reichert B. E.: *Structures of ZrO_2 polymorphs at room temperature by high-resolution neutron powder diffraction.* Acta Crystallogr. B: Struct. Sci. **44**, 116 (1988)

[20] Teufer G.: *The crystal structure of tetragonal ZrO_2.* Acta Cryst. **15**, 1187 (1962)

[21] Gómez-García D., Martínez-Fernández D., Domínguez-Rodríguez A., Castaing J.: *Mechanisms of High-Temperature Creep of Fully Stabilized Zirconia Single Crystals as a Function of the Yttria Content.* J. Am. Ceram. Soc. **80**, 1668 (1997)

[22] See e.g. *Numerical Recipes: The art of scientific computing.* – Press *et al.*, (Eds.), Cambridge University Press, New York, 1990

[23] Troullier N., Martins J. L.: *Efficient pseudopotentials for plane-wave calculations.* Phys. Rev. B **43**, 1993 (1991)

[24] Perdew J. L., Burke K., Ernzerhof M.: *Generalized Gradient Approximation Made Simple.* Phys. Rev. Lett. **77**, 3865 (1996)